

We are IntechOpen, the world's leading publisher of Open Access books Built by scientists, for scientists

6,900

Open access books available

186,000

International authors and editors

200M

Downloads

Our authors are among the

154

Countries delivered to

TOP 1%

most cited scientists

12.2%

Contributors from top 500 universities



WEB OF SCIENCE™

Selection of our books indexed in the Book Citation Index
in Web of Science™ Core Collection (BKCI)

Interested in publishing with us?
Contact book.department@intechopen.com

Numbers displayed above are based on latest data collected.
For more information visit www.intechopen.com



Scale-Up and Optimization for Slurry Photoreactors

*Gianluca Li Puma, Fiderman Machuca-Martínez,
Miguel Mueses, José Colina-Márquez
and Ciro Bustillo-Lecompte*

Abstract

Several aspects of scale-up and optimization of heterogeneous photocatalytic reactors are detailed in the following chapter. The relevance of the dimensionless numbers, the critical factors of the photoreactor design, and the optimization methods are explored from an engineering point of view. The apparent optical thickness is the most crucial dimensionless parameter for photoreactor design and optimization; therefore, the study will be more focused on this topic. Moreover, a real case for a commercial application of the solar photocatalysis will be presented in this chapter. This full-scale plant is currently operating as an industrial wastewater treatment plant in a flexographic company located in Cali, Colombia.

Keywords: scale-up, heterogeneous photocatalysis, full-scale, advanced wastewater treatment

1. Introduction

For scaling-up heterogeneous photocatalytic reactors, it is necessary to consider the following key factors: kinetic law, UV radiation source, photoreactor type, catalyst type (suspended or fixed), and mass transfer phenomena. The performance of the photocatalytic reactor depends directly on the number of photons absorbed by the catalyst surface; and this is related to the geometry of the photoreactor, UV photons source, and how the catalyst interacts with the chemical species. Although the photoreactor models consider practically all these aspects, the use of dimensionless parameters is highly recommended for scaling-up purposes. The four dimensionless numbers needed for the scaling-up process are as follows [1]:

- Reynolds number (N_{Re}), which suggests the type of fluid regime to be considered for the reactor model.
- Damkohler number (N_{Da}), which expresses the ratio of the overall reaction rate, calculated at the inlet concentration and at maximum photon flux, to the maximum input mass flow rate of the reactant model (laminar or turbulent flow) to be included in the model. The values estimated for this dimensionless number allow identifying which can be the slower stage of the overall reaction rate.

- The optical thickness of the photoreactor (τ), corresponding to the degree of opacity of the photoreactor.
- The scattering albedo of the photocatalyst (ω), which depends on the optical properties of the catalyst.

The last two dimensionless numbers (optical thickness and scattering albedo) are the most relevant for scaling up photocatalytic reactors. Both help to describe the dynamics of the UV photon absorption and determine the level of difficulty of the scaling-up process. For example, some thin-film slurry (TFS) photoreactors (**Figure 1**) can exhibit very low values of scattering albedo ($\omega < 0.3$); thus, the rate of photon absorption (LVRPA) can be estimated by neglecting the scattering effect safely, and the scaling-up process can be more straightforward for this case; whereas, for TFS with higher scattering albedos or “geometrically thick” slurry photoreactors, such as compound parabolic collectors (CPC) and tubular reactors, the LVRPA needs to be modeled with more complex mathematical expressions due to the scattering effect cannot be neglected [1].

Although TFS reactors with low scattering albedos are easier to scale-up (regarding photonic effects calculations), they can result not so practical when they need to handle larger volumes of reaction, especially if the dimensionless numbers need to remain constant in the process of scaling-up. Several aspects of scale-up and optimization of heterogeneous photocatalytic reactors are detailed in the following sections of this chapter.

2. Scale-up of heterogeneous photocatalytic reactors

The dimensions of a full-scale TFS reactor can be challenging to handle if, for example, a large plate of several meters of length and width needs to be located in a reduced space. This is not the case for CPC or tubular photoreactors, which can be set up as modular units for larger reaction volumes. This advantage is more relevant when the photon source is the UV solar radiation since the photocatalytic reactors must be located outdoors, and the TFS reactors must have additional protection for weather phenomena. The solar CPC photoreactors, instead, are more robust, and there are several large-scale applications as it has been reported in the literature [1–5].

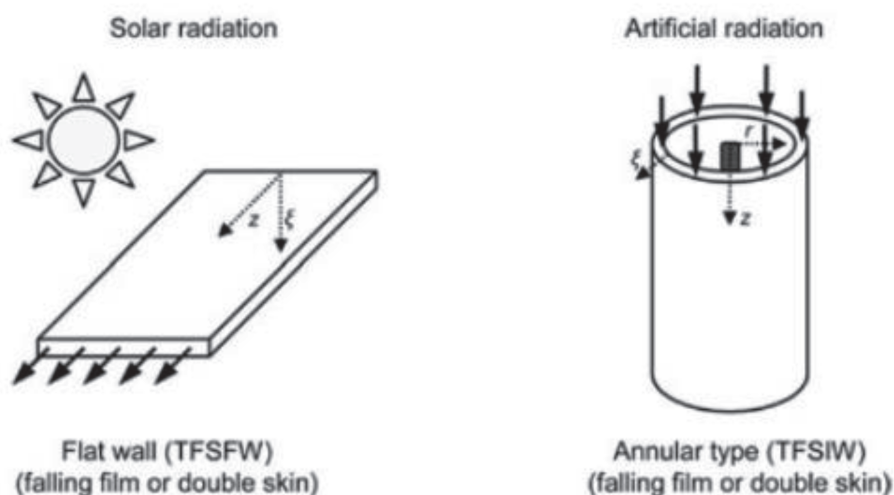


Figure 1.

Thin-film slurry (TFS) photoreactors. © 2005 Elsevier Science Ltd. Originally published in Li Puma [1] under CC BY-NC-ND 4.0 license.

Nonetheless, other “geometrically thick” reactors can be considered as feasible options to be scaled-up, regarding the cost-benefit ratio.

The optical thickness, which depends on the catalyst load and the reactor thickness, may be manipulated in order to maximize the photon absorption by the catalyst. Consequently, it is necessary to observe how the LVRPA behaves with different values of optical thickness, considering that the type of reactor is relevant to the behavior of this parameter.

Figure 2 shows how the conversion of an ideal substrate varies with the optical thickness and the type of reactor: falling film laminar flow (FFLF), plug flow (PF), and slit flow (SF) reactors. It is also clear that the lower scattering albedos allow higher conversions of this ideal substrate.

The “optically thick” reactors ($\tau > 1.0$) exhibit lower conversions due to a high scattering effect although there are also high photon absorption rates due to the higher amounts of catalyst. For this kind of photoreactors, the optimization of the apparent optical thickness is strongly recommended in order to use the minimum amount of catalyst that ensures satisfactory performance of the photocatalytic reactor.

Other dimensionless numbers or parameters can be used. The dimensionless intensity of radiation at the entrance window of the reactor and the dimensionless LVRPA may be useful as well. The following expressions apply for TFS reactors ($\omega < 0.3$) [1]:

$$I_{\xi^*=0, \tau^*}^* = \frac{I_{\xi^*=0, \tau^*}^{\xi^*=0}}{\left(I_{\xi^*=0}^{\max}\right)_{\omega=0}} \quad (1)$$

$$LVRPA^* = I_{\xi^*=0, \tau^*}^* \exp(-\tau_{app} \xi^*) \quad (2)$$

where $I_{\xi^*=0, \tau^*}^*$ is the dimensionless intensity at the entrance window ($\xi^* = 0$); $I_{\xi^*=0, \tau^*}^*$ is the actual intensity estimated at the entrance window; and $\left(I_{\xi^*=0}^{\max}\right)_{\omega=0}$ is the maximum intensity of the radiation estimated in the absence of scattering effects.

The dimensionless LVRPA is easily estimated from the dimensionless intensity at the entrance window, the apparent optical thickness (τ), and the dimensionless

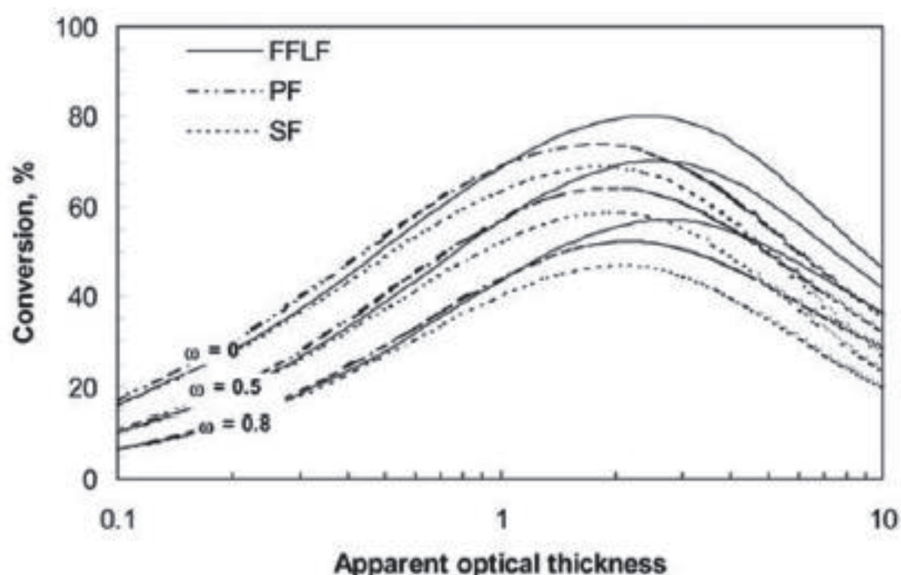


Figure 2. Model simulations for the conversion of a substrate as a function of the optical thickness and scattering albedo for different idealized flow conditions. © 2005 Elsevier Science Ltd. Originally published in Li Puma [1] under CC BY-NC-ND 4.0 license.

radial coordinate (ξ^*). As mentioned earlier, the problem with those expressions is that they are limited to cases where the scattering albedo is low. However, that is not the case for the commercial TiO_2 used in heterogeneous photocatalytic reactions, which exhibits higher values of ω [1].

The dimensionless intensity can be used when a photocatalytic reactor with artificial UV radiation source is going to be scaled-up. Nevertheless, this expression cannot be applied for solar photoreactors because of the variability of the solar incident radiation. For this case, the LVRPA must be calculated based on the solar radiation emission models, considering the location latitude, time, and date and the clearness factor (K_C) [2]. This K_C parameter depends on the number of clouds at the time of the photocatalytic reaction, which varies on the weather conditions [3].

3. Optimization methods

The optimization for photocatalytic reactors is usually intended for finding the operating conditions that ensure the best performance regarding the degradation of a specific substrate by photochemical oxidation. For the scaling-up process, this is a necessary step for making the heterogeneous photocatalysis a profitable and competitive technology.

The optimization can be carried out from the experimental data of pilot-scale photoreactors by using a simple empirical model. This model is built from a polynomial expression that involves the most relevant operating variables that affect the interest variable (e.g. relative degradation of the substrate).

Figure 3 shows an example where the surface response methodology was used for optimizing the decolorization of methylene blue (MB) with two bench-scale photoreactors [6].

In the reported study by Arias et al. [6], the tubular reactor corresponds to a 38 mm-ID borosilicate glass tube of 30 cm of length (**Figure 4a**), whereas the CPC reactor consists of the same glass tube but with a reflective collector that redistributes the reflected radiation (**Figure 4b**).

For each case, the slurry was recirculated during 30 min under darkness conditions, in order to achieve the adsorption equilibrium of the dye on the catalyst surface. In previous results, the adsorption removal of the dye was around 10–15%. It was possible to build the polynomial models from results of a full-composite experimental design, where the TiO_2 load and the initial pH of the slurry were selected as the controllable factors and the relative decolorization was the response variable. The optimization was made by using the first-derivative method for the

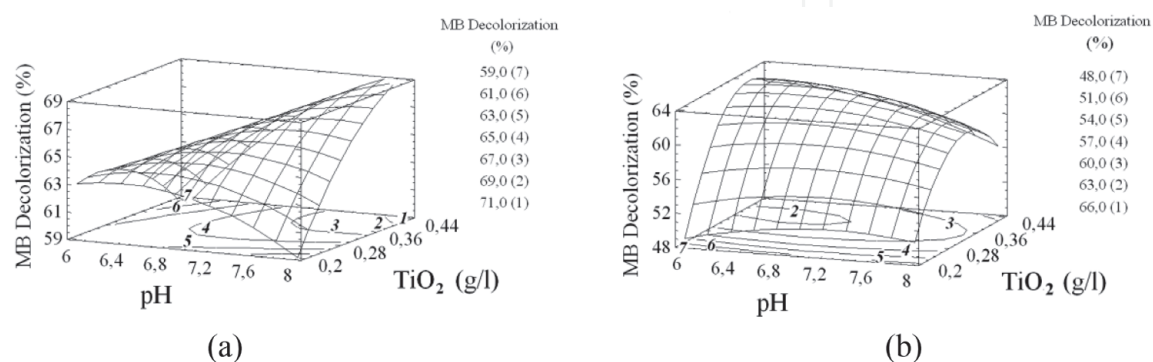


Figure 3. Surface response plots and contour lines for methylene blue (MB) TiO_2 -based photocatalytic degradation: (a) CPC reactor and (b) tubular reactor. © 2005 Walter de Gruyter & Co. Originally published in Arias et al. [6] under CC BY-NC-ND 4.0 license.

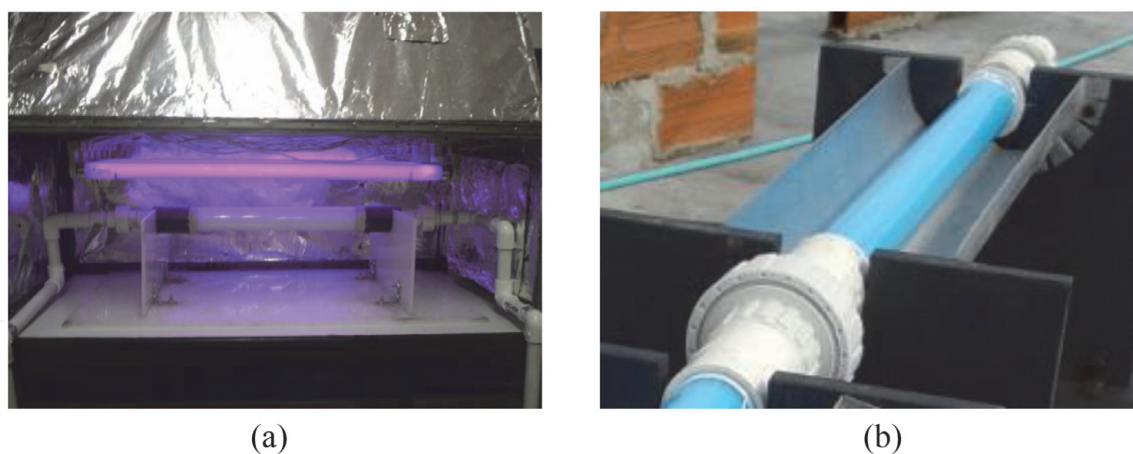


Figure 4.
 Bench-scale photoreactors used for MB decolorization; (a) tubular and (b) CPC.

obtained empirical expressions, and the optimal catalyst load and pH were found for each photoreactor [6].

This method allows finding optimums without a significant mathematical effort; however, its results only are scalable within the experimental conditions used for the pilot or bench-scale tests. Besides, the effects of mass transfer and the photon absorption effects are not considered in this empirical model. This leads to using of photoreactors of the same dimensional and hydrodynamic features than that used for the experimental tests. Therefore, this optimization method is limited because of its empirical nature, and it is necessary to consider a method that involves dimensionless numbers, more suitable for scaling-up.

The other method consists of optimizing the mathematical expressions of the photoreactor model. The first derivative (as optimization tool) might not be practical for finding the maximums or minimums of these mathematical expressions due to their intrinsic complexity, especially for “geometrically thick” photoreactors. Therefore, it is more recommendable to evaluate the property to be optimized in a wide range of the dependent variables. Despite the demanding calculation time of this type of optimization, this strategy is more applicable for the scaling-up process since the use of dimensionless numbers in the optimization ensures the similarity between scales.

The most suitable dimensionless parameter being used in the optimization is τ . Generally, the variable to be optimized is the volumetric rate of photon absorption (VRPA). However, the degradation of a specific substrate can be further used.

Figure 2 shows the behavior of a hypothetical conversion vs. the apparent optical thickness and the plots that exhibit an optimum.

From the LVRPA expression and supposing a constant UV radiation flux (I_0) of 30 W/m^2 , the following plots can be obtained in order to optimize the rate of photon absorption in the CPC or tubular reactors (**Figure 5**).

The plots shown in **Figure 6** describe the behavior of the VRPA/H with tubular and CPC reactors of 32 mm ID and AEROXIDE® P-25 as the catalyst. From the previous definitions, these reactors are considered “optically thick,” and the LVRPA must be calculated using the six-flux model (SFM) approach. It is important to note that these plots are only applicable to the conditions of radiation and the tube diameter specified [7]. Although for scaling-up modular photoreactors, such as the CPC or tubular, the tube diameter can remain constant in the process. In the case of different diameter (or different reactor thickness), τ is the most suitable parameter to be involved in the optimization. **Figure 6** shows a similar trend to the one shown in **Figure 2**. The presence of optimums in each case is because of the scattering increases with the optical thickness, generally associated to the high catalyst loads that do not permit a satisfactory light penetration inside the reactor bulk.

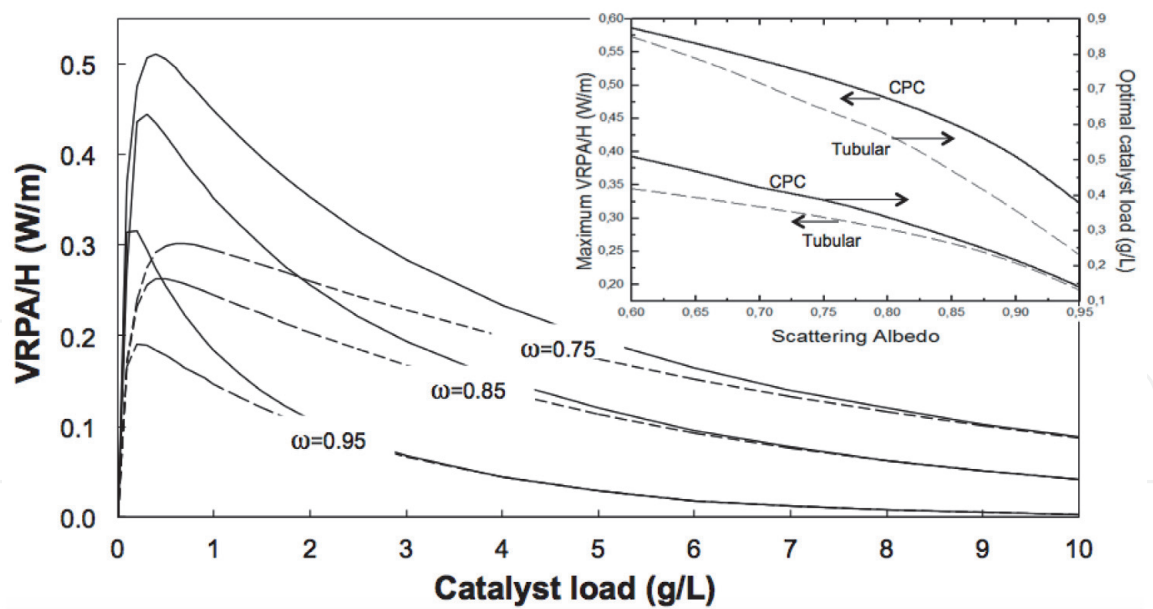


Figure 5. Volumetric rate of photon absorption per reactor length unit (VRPA/H) vs. TiO_2 catalyst load; dashed line, tubular, and solid line, CPC reactor, with 30 W/m^2 of incident UV radiation flux. © 2010 American Chemical Society. Originally published in Colina-Márquez et al. [7] under CC BY-NC-ND 4.0 license.

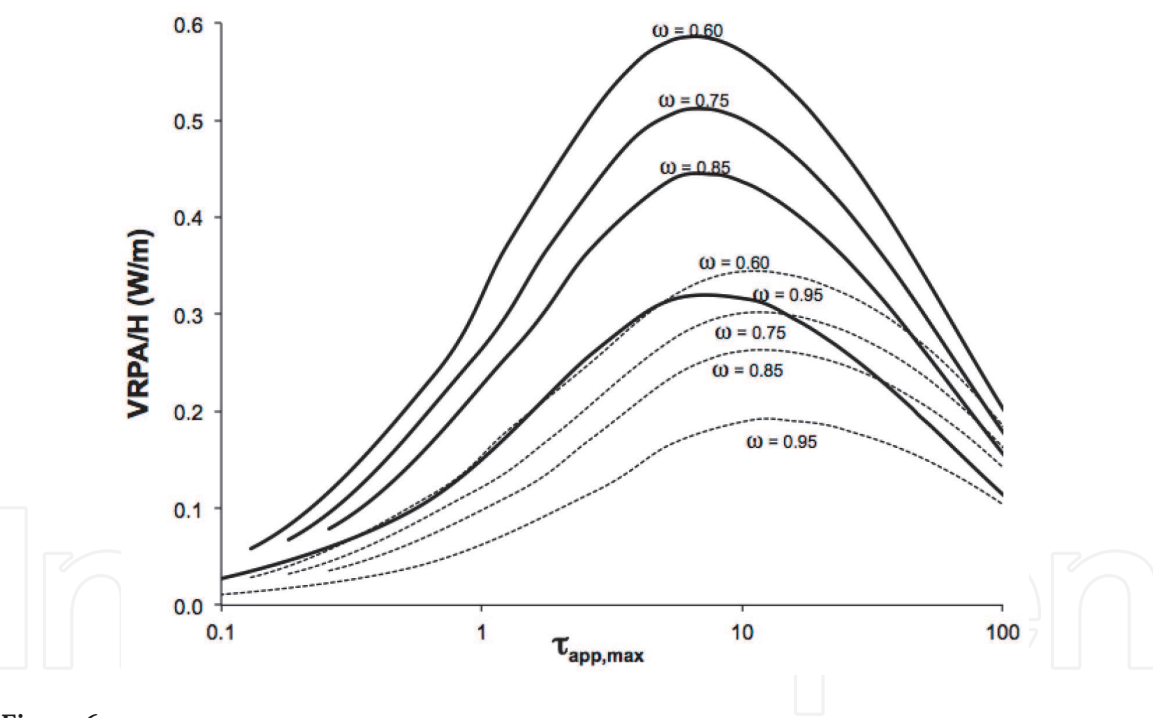


Figure 6. Volumetric rate of photon absorption per reactor length unit (VRPA/H) vs. apparent optical thickness; dashed line, tubular and solid line, CPC reactor, with 30 W/m^2 of incident UV radiation flux. © 2010 American Chemical Society. Originally published in Colina-Márquez et al. [7] under CC BY-NC-ND 4.0 license.

4. Design criteria

4.1 Preliminary considerations

The design of full-scale photocatalytic plants keeps several similarities with the design of conventional plants. It is essential to consider the following parameters before starting to make the engineering calculations for the photocatalytic plant:

- Type of reactor and reactor geometry.

- Type of process regime (batch or continuous).
- Photon source (artificial or solar).
- Catalyst (supported or slurry).
- Oxygen supply (artificial or natural).
- Total handled volume.

Considering the amount of data and information gathered during the pilot-scale tests, the most relevant aspects of the plant design must be detailed in this phase.

4.1.1 Type of reactor

The selection of the photoreactor is determinant for the photocatalytic performance. The rate of photon absorption is directly related to the type of photoreactor and construction materials. The selection depends on the type of photon source and the type of catalyst as well. A reactor with a fixed catalyst can have different geometry and specifications than a slurry reactor. The same considerations apply for solar photoreactors and artificial UV-based ones.

4.1.2 Type of regime

The type of regime defines, among other parameters, the size of the photocatalytic reactor. The plant size for a batch regime is usually larger than the size of a continuous regime; nonetheless, most of the literature about photocatalytic reactors [8–10] has been focused on the batch and the semi-batch regimes. This is generally associated with the small volumes (1–100 L) handled by the pilot-scale photocatalytic reactors.

4.1.3 Photon source

The UV photon sources can be from UV-lamps (artificial) or the sun (natural). The main advantage of the UV-lamps is that they supply a constant flux of radiation, but their energy consumption supposes an additional cost for the operation of a full-scale plant. whereas, the solar radiation is a cheap and abundant form of UV photon supply (depending on the location). However, the radiation flux is highly variable, and it is only available during the daytime hours.

4.1.4 Catalyst

The fixed catalyst does not need to be separated in a later stage of the process, but it has mass transfer and photon absorption limitations; whereas the slurry catalyst can be more effective (especially for photon absorption effect), but it needs an additional separation stage that increases the costs for a full-scale plant.

4.1.5 Oxygen supply

The concentration of dissolved oxygen in water must be kept near to the saturation in order to avoid slower oxidation rates in the photocatalytic process. This oxygen can be supplied by the free contact of the falling stream with the atmospheric air, or with an air compressor with a sparging device. The free contact can

be more suitable with small volumes, where the flow rate supplies enough turbulence to favor the vigorous contact between the water and the atmospheric air. Otherwise, the installation of an air compressor with the corresponding sparging system would be mandatory.

4.1.6 Total volume

One of the limitations of the heterogeneous photocatalysis, aimed for wastewater treatment, is the total volume handled by the reaction system. The larger volumes require larger installed areas for the photoreactors. Although the size of the plant depends on the kinetics of the photocatalytic reaction, the total volume determines the final dimensions of the full-scale plant.

4.2 Photoreactor selection

The criterion for selecting a reactor type considers two main aspects: performance and cost. The pilot-scale tests must provide the required information about these two features. Although we can find a wide variety of lab-scale and pilot-scale photocatalytic reactors in the scientific literature, we must ensure that the selected reactor is commercially available for full-scale applications or at least its assembling costs are affordable.

The photoreactors shown in **Figure 7** can use artificial or solar radiation as a UV photon source, except for the annular reactor that only can use artificial UV

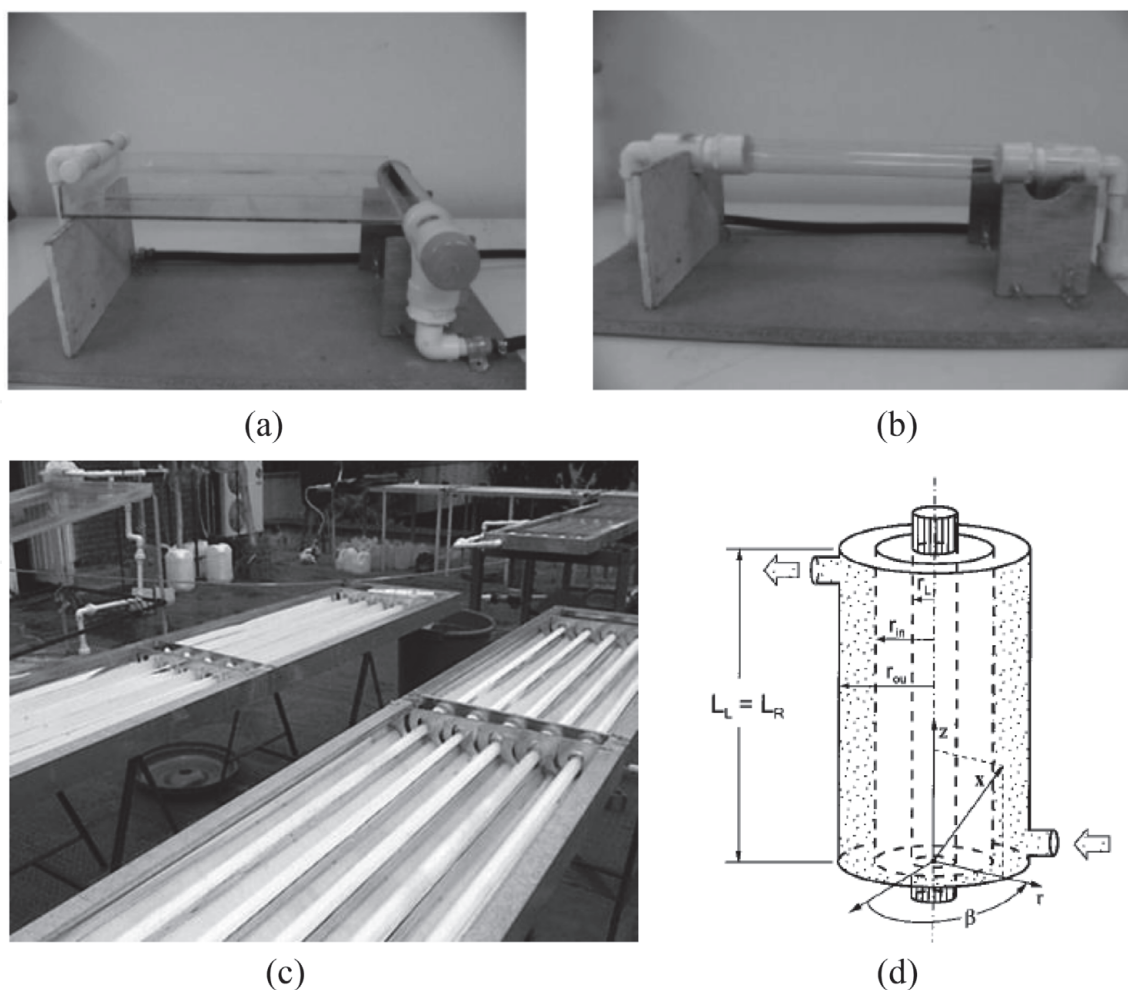


Figure 7. Photocatalytic reactors: (a) flat plate, (b) tubular, (c) CPC, and (d) annular. © 2010 American Chemical Society. Originally published in Romero et al. [11] under CC BY-NC-ND 4.0 license.

radiation. Besides, catalysts can be used as slurry or fixed plates in any of the depicted reactors. Regarding the selection of the UV-photon source, the suggested strategy consists of decreasing costs by using solar radiation whenever is possible. If the solar radiation is feasible as a UV photon source, the photoreactor should be selected based on its performance, considering the variability of the radiation intensity.

4.2.1 Tubular reactor

Figure 7b shows a bench-scale tubular reactor. This reactor geometry is quite simple because it only consists of a tube made of a material with good UV radiation transmittance. As the catalyst is usually used as slurry, this reactor must operate under the turbulent regime in order to avoid that the catalyst precipitates.

This technology can receive direct and diffuse solar radiation on the reactor part that is directly exposed. However, some disadvantages can appear due to the soiling or the reactor wall due to the catalyst, such as mass transfer limitations and a low photon penetration inside the reactor bulk [11].

4.2.2 Compound parabolic collector (CPC)

The compound parabolic collector (CPC) consists of two reflective screens located at the bottom of the tubular reactor [12]. These reflective screens are able to reflect the radiation to the bottom of the reactor, which improves the performance of this reactor over the tubular reactor (without collectors). The CPC configuration is one of the most used in reactors for solar applications [4, 5, 13, 14]. These collectors can redistribute the radiation and reflect it without concentrate, avoiding that the fluid temperature increases [15]. This reactor uses the diffuse and direct solar radiation as a UV photon source.

Figure 8 depicts the manner how solar radiation can be redistributed around the tubular receiver surface without concentrating the radiation. The equations that describe the curvature of the involute are as follows:

$$x_{CPC} = \pm R_R (\sin t - t \cos t) \quad (3)$$

$$y_{CPC} = -R_R (\cos t + t \sin t) \quad (4)$$

where x_{CPC} and y_{CPC} are the rectangular coordinates of an involute given point, R_R is the inside reactor radius, and t is a parameter that takes values from 0 to 2π radians.

4.2.3 Tilted flat plate

The tilted flat plate reactor is also known as the falling film reactor, and it does not have concentrators. Because of its simplicity and low-cost construction, it is one

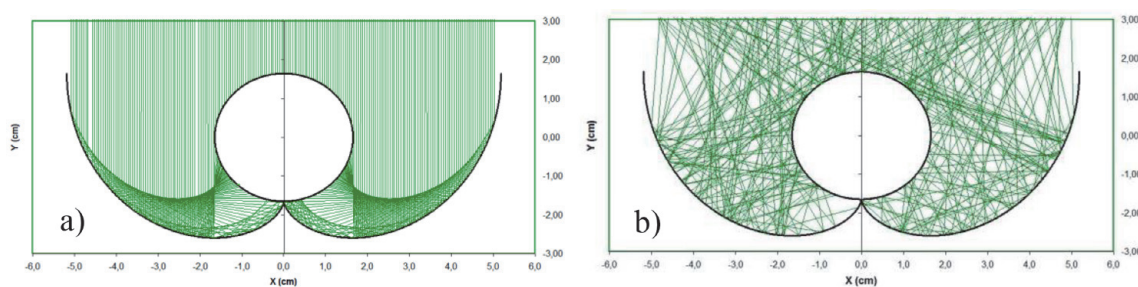


Figure 8.
 Solar radiation modeled with the ray-tracing technique: (a) direct radiation and (b) diffuse radiation.



Figure 9.
Pilot-scale solar flat plate reactor used for degradation of a model pollutant.

of the most used reactors for pilot-scale studies. **Figure 9** shows a solar flat plate with a supported catalyst. The main advantage of this configuration is that the entire falling film is exposed to solar radiation with no barriers. The optical thickness is smaller than the one observed in the tubular and the CPC reactors, which permits using higher catalyst loads and achieving better photon absorption rates. However, the most significant drawback of this type of reactor is the larger area occupied compared to that used in tubular reactors. In addition, there is no possibility of setting up this photoreactor like a modular unit because it would require a pump for each module.

4.2.4 Comparison of photoreactor configurations

The selection of the most suitable photoreactor depends not only on the reactor performance but also on its potential for being scaled-up. Moreover, the type and the concentration of the substrate are determinant for the photocatalytic reactor performance. A comparative assessment can provide useful information in order to make the right decision. This means that the pilot-scale tests must be carried out under the same operating conditions, or at least under very similar ones than the expected conditions of the full-scale plant.

Previous reports about photoreactor comparisons have been carried out with artificial UV-based and UV solar-based systems [16–19]. Bandala et al. [17] study focused on the comparison of several solar tubular reactors with different types of collectors and without collectors for oxalic acid degradation. Although there was no significant difference between the performances of the photoreactors with collectors, their performance was higher than that of the photoreactor without collectors.

Figure 10 shows a case where a robust experimental design was used for showing the performance of three different solar photoreactors in the degradation of a mixture of commercial pesticides. This criterion for choosing the more suitable reactor was based on the higher signal-to-noise ratio exhibited. The signal is the overall photocatalytic removal, and the noise is the noncontrolled parameter that affects the performance significantly. This noise parameter corresponds to the accumulated UV solar radiation within a fixed time lapse.

In short, the most robust photoreactor was the flat plate, followed very closely by the CPC. This means that the selected reactor would be the flat plate for this case; however, there is a critical drawback for this reactor: a large flat plate would be needed for treating higher volumes of polluted wastewater. Therefore, the scaling-up of the flat plate would be impractical, and the best option would be then the CPC

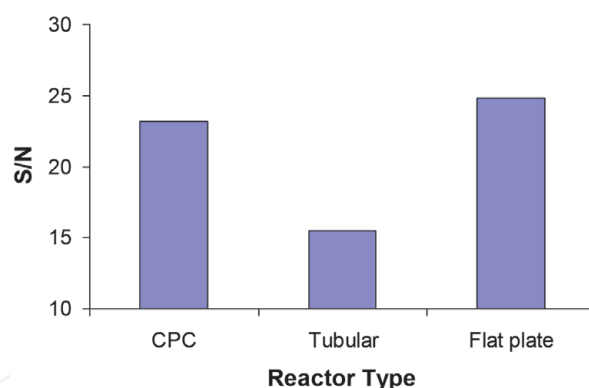


Figure 10.
 Signal-to-noise ratio (S/N) for pesticides degradation with three different solar photoreactors.

reactor. Additionally, this photoreactor can be used in modules, which can be mounted or dismounted easily.

4.2.5 Selection of construction materials

The construction materials can vary depending on the reactor geometry and type. Nonetheless, all the materials considered must fulfill a common condition: they must be resistant to the atmospheric corrosion or at least, they must have protection against this phenomenon. In the case of outdoor plants, such as the solar photocatalytic reactors, the materials must resist prolonged solar radiation exposition or not undergo photodegradation under these conditions.

For photoreactors with tubular geometry, the optical properties of the construction material of the reactor must ensure the maximal use of the available photons that reach the reaction space. Regarding this aspect, the material must permit the free pass of the UV photons through it. This means that must have a high transmittance within the UV absorption range of the catalyst (e.g., 275–390 nm for the commercial P25 TiO₂).

Figure 11 shows the transmittance of different materials used in photoreactors. According to Cassano et al. [20], the material with the best transmittance is the quartz, but commercial applications with this material would be expensive. The most feasible is then the borosilicate glass with low contents of iron (Pyrex® and Duran® commercial brands). However, polytetrafluoroethylene (PTFE) can be a cheaper option with comparable transmittance respect to the borosilicate glass.

4.3 Pilot-scale plant considerations

Figure 12 shows an example of a pilot-scale plant with a TiO₂-based LFFS photocatalytic reactor aimed to degrade salicylic acid [21]. The kinetic law and the mass balance can be estimated from the concentrations measured at the sample ports and the proposed model for this photocatalytic reactor. The feed tank must be kept continuously agitated in order to maintain a uniform distribution of the concentration. Furthermore, it is essential to ensure a constant oxygen supply for avoiding that the photochemical reaction rate decreases because of the oxygen consumption. The following features must be considered for full-scale plant design:

- Type, geometry, and construction materials of the photocatalytic reactor must remain the same for a full-scale plant.
- Fluid regime (Reynolds number must be kept as constant).

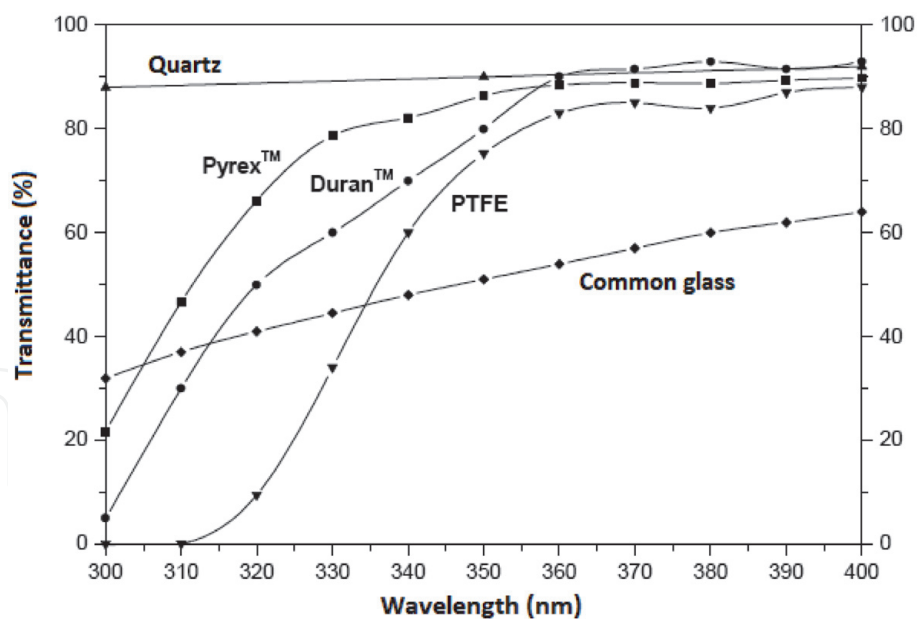


Figure 11.
Transmittance of different materials used in photoreactor design.

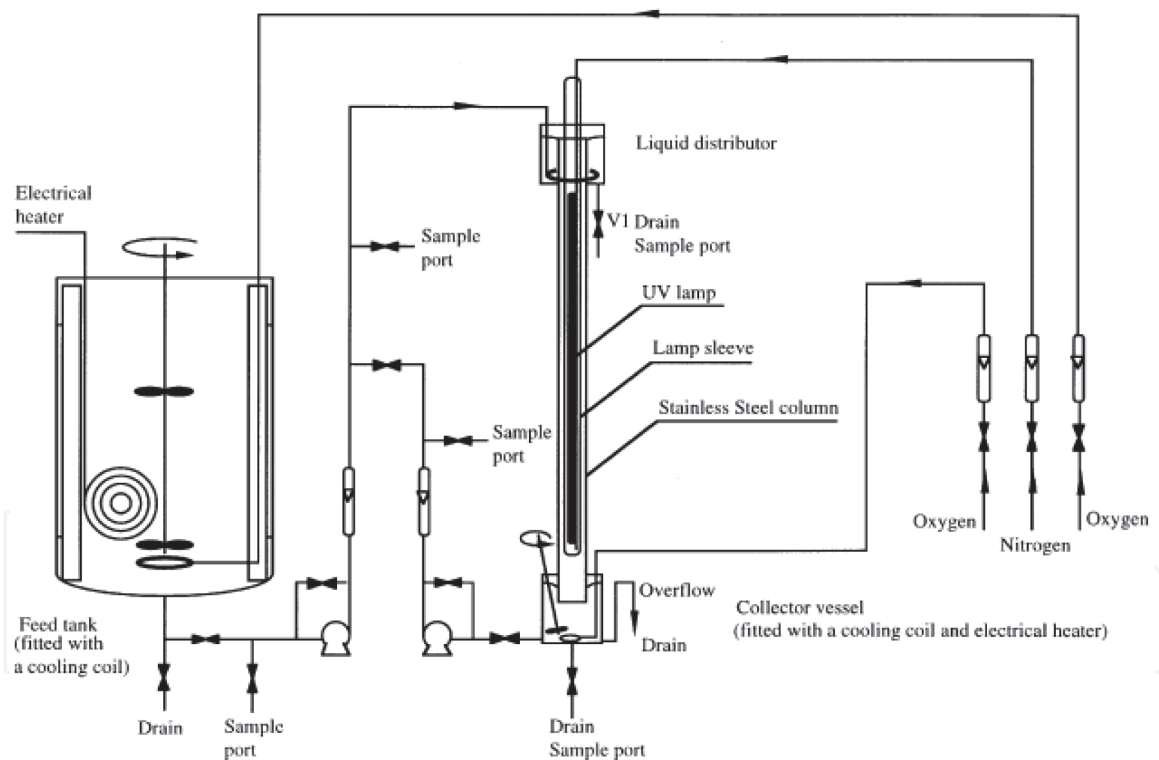


Figure 12.
Pilot plant for a laminar flow falling film slurry (LFFS) photocatalytic reactor. © 1998 Elsevier Science Ltd. Originally published in Li Puma and Yue [21] under CC BY-NC-ND 4.0 license.

- Sampling ports located at relevant streams for collecting information about substrate concentrations along the process.
- Instruments and process control for obtaining data of the operating variables such as temperature, UV radiation, pH, and dissolved oxygen.
- Easy operation.

Although the temperature may not vary significantly during the tests, it is recommendable to include cooling or heating systems for controlling the temperature, especially with systems that use UV artificial light as a photon source. Regarding the pH, it is not necessary to control it. Besides the tremendous difficulties for controlling the pH, the improvement in the photocatalytic reactor performance is not considered significant enough.

4.3.1 Plant layout

The full-scale plant can resemble the pilot-scale plant in many aspects; however, there are other stages of the process that need to be considered. Despite the process simplicity, details such as the auxiliary equipment, pumping, and storage tanks cannot be underestimated.

The photocatalytic plants are aimed usually for wastewater treatment. Thus, the final product plant (the treated water) can be reused or spilled on the surface water bodies. This aspect must be considered in the plant layout (e.g., temporal storage tanks or pipelines for conducting the treated water to its final destination). Another essential feature is the catalyst recovery. Since the catalyst is used as a slurry in most of the cases, a separation-recovery subprocess should be considered.

Figure 13 shows the isometric drawing of a demonstration plant where 2 m³ of wastewater polluted with NBCS were treated. It is recommended to simplify the subprocess for recovering the TiO₂ because of the installation and operation costs of a full-scale plant increase significantly. It is essential to specify the pump size correctly and consider the discharge pressure in order to avoid leaks or tubes breakage. As seen in the plant layout depicted in **Figure 13**, the modules were set up in two rows of 21 reactors each. This was done to reduce the pressure at the tube's joints, but the Reynolds number must remain constant to avoid mass transfer limitations [22].

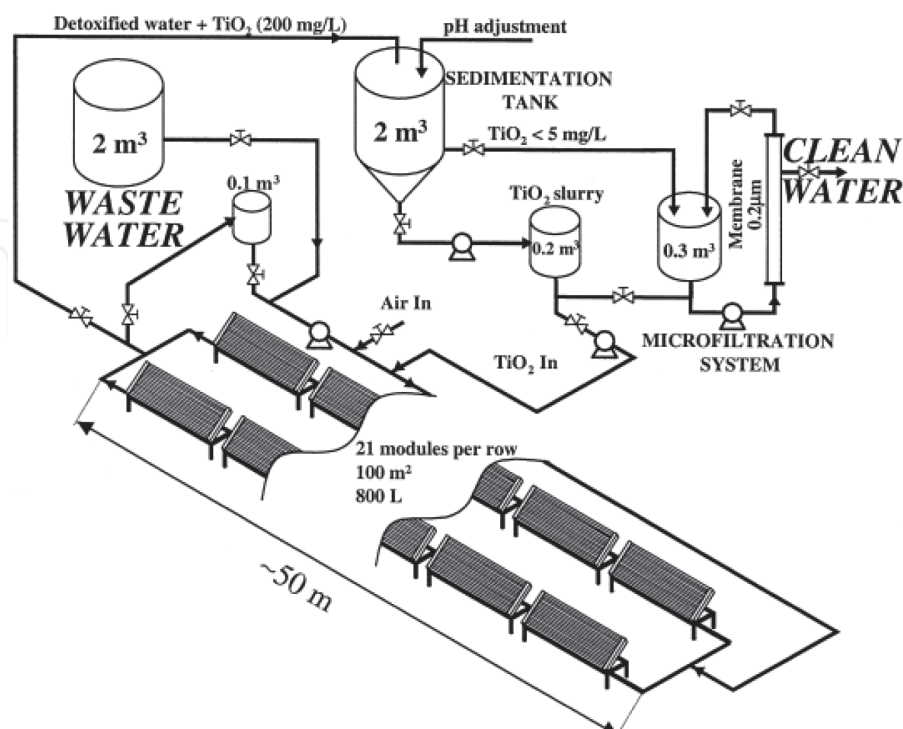


Figure 13. Isometric drawing of a demonstration solar photocatalytic plant for treatment of water contaminated with non-biodegradable chlorinated solvents (NBCS). © 1999 Elsevier Science Ltd. Originally published in Blanco et al. [22] under CC BY-NC-ND 4.0 license.

4.4 Design, assembly, and operation of a full-scale solar photocatalytic plant

This section presents the main aspects that were considered in the construction and the operation of a full-scale solar photocatalytic plant for treating industrial wastewater from a flexographic industry. This full-scale plant is the first commercial solar photocatalytic installation in America.

Previous studies on laboratory and pilot-scale photoreactors were conducted to determine the technical feasibility of using photocatalysis as a viable treatment of 2 m³/d of water contaminated with industrial dyes, and consequently, it served as the basis for a technology-transfer deal with the company and a patent application [23, 24].

4.4.1 Background and description of industrial process

A major company in Colombia that manufactures notebooks was facing issues with the treatment of the wastewater produced after washing the rolls used for printing the lines of the notebooks. This residual effluent was contaminated with the industrial dye, which has proven to be resistant to biological treatments. Therefore, it was necessary to apply a novel technology (such as heterogeneous photocatalysis) that could ensure the color removal.

The primary objective was the reuse of the treated water for washing the printing rolls. The most important innovation of this photocatalytic process was the simple way in which the solid catalyst is reused without using complex and expensive systems to recover after each treatment process. The use of solar radiation was another significant advantage since the location has good solar light availability.

The process flow diagram of the full-scale solar photocatalytic plant is shown in **Figure 14**. This scheme can be used for different kinds of wastewater and which can be treated by photocatalysts. This photocatalytic process was applied for treating industrial residual wastewaters contaminated with recalcitrant compounds, in this case, flexographic dye residues. The industrial wastewater is generated from washing the printing rolls soiled with dye residues after a typical work cycle. This wastewater is collected in the tank T-1 and then pumped to the recycling-feed tank

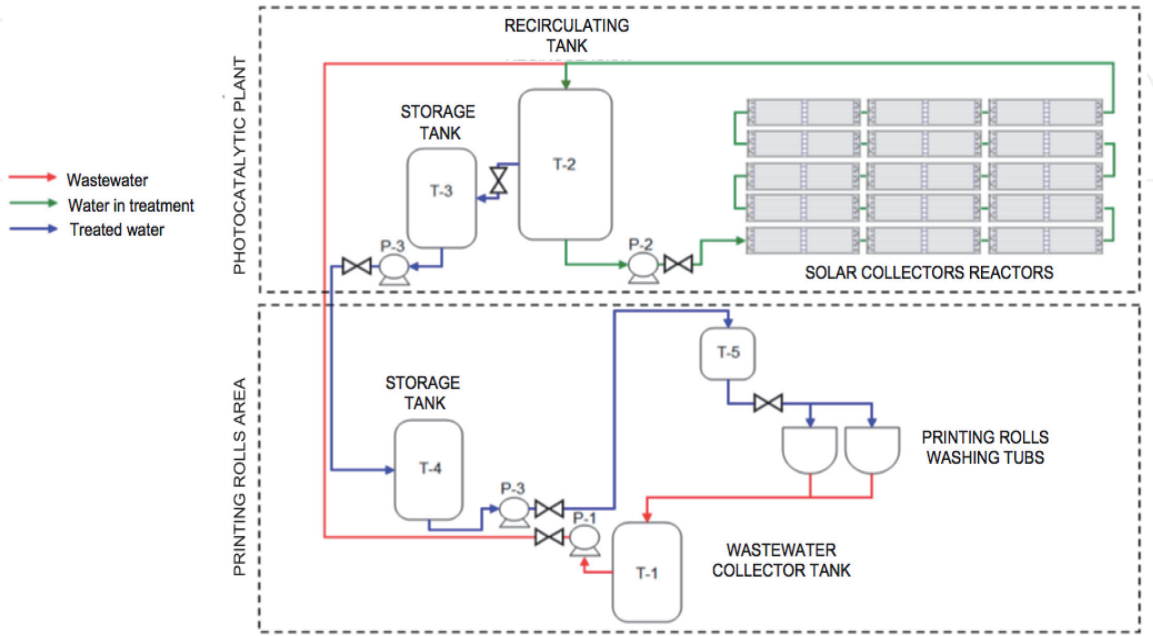


Figure 14.
Process flow diagram of the full-scale wastewater treatment photocatalytic plant.

T-2 using the pump P-1. The wastewater stored in this tank is diluted with water in a ratio of 4:1. The first dilution of the process was made with fresh water; after that, treated water is used for this purpose. Once the tank was full, the catalyst was added for the first and the only time as far. The same catalyst has been reused in the subsequent treatments, since the plant started up in September 2009, and it will be removed when it has lost its activity.

The pump P-2 recirculates the slurry through the CPC photoreactors. As it was previously mentioned, the process has an average duration because it depends on the availability of solar radiation. The process is suspended under the following conditions: color removal from the contaminated effluent, adverse weather conditions (hard rain or strong winds), or if the sun has set. In case of the color removal, the next step is the catalyst settled down in order to separate the clear supernatant. This process lasts between 12 and 24 h, depending on the amount of treated water to be reused to wash the rollers.

Between 10 and 25% of the treated water from the recirculation tank T-2 are transferred by gravity to the intermediate storage tank T-3. When this tank has enough volume (1.5–2.5 m³), the treated water is pumped via P-3 to the secondary storage tank T-4. Finally, according to plant requirements, it is pumped via P-4 to the tank T-5, which is used to provide clean water for washing the soiled printing rolls, thus closing the treatment cycle [24].

4.4.2 Design of pilot solar photoreactor model

Each photoreactor module comprises 10 tubes placed in five rows over the CPCs (**Figure 15**). The glass tubes are 32 mm ID and 1.4 mm of thickness manufactured by Schott Duran®. The tubes were cut from their original length of 1.5 m to 1.2 m in order to correspond the length of the sheets used for constructing the collectors. The tubes diameter must be selected between 25 and 50 mm, since diameters smaller than 25 mm are not feasible because of pressure drop limitations; whereas, diameters larger than 50 mm present photon absorption issues due to a significant photon scattering.

The collectors were constructed in high-reflectivity aluminum (80–90% of reflectivity), which should be weather resistant as well. The involutes, characteristic of the CPCs, as seen in **Figure 15**, were molded using a folding machine based on

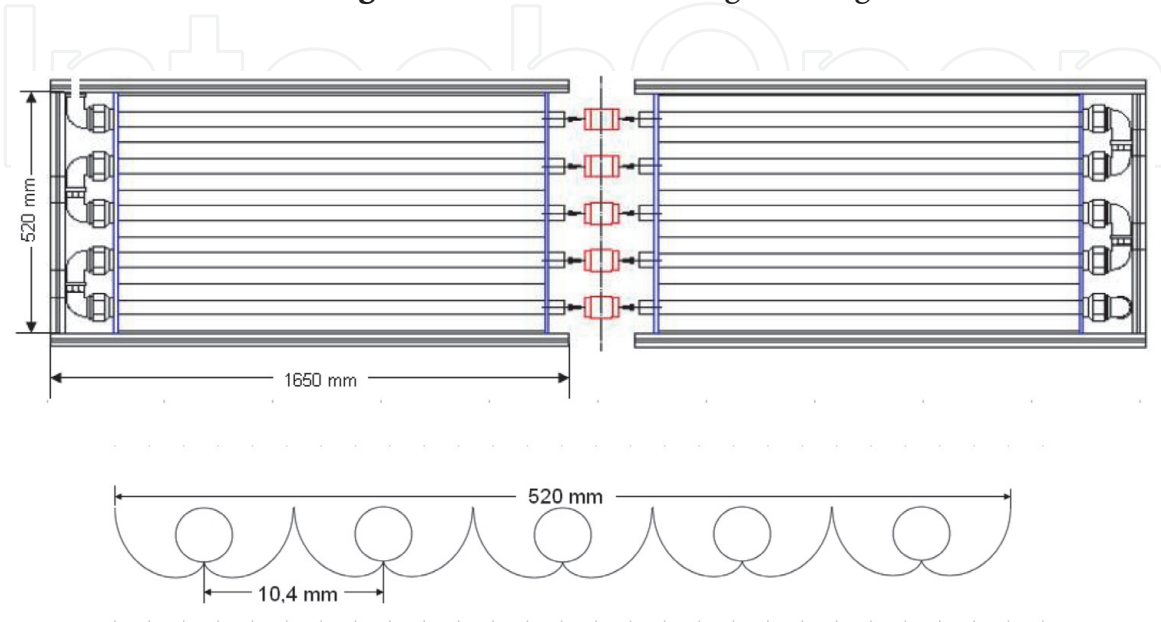


Figure 15.
 Main structure of the CPC photoreactor type and cross section of tubes and manifolds for CPC.

numerical control. The supporting structure was constructed with galvanized zinc sheets, as well as the guides that supported the collectors and the glass tubes. Between the glass tubes, anti-slip PVC joints were located (red-colored joints shown in **Figure 15**), which could permit torsion without damaging the glass tube during maintenance processes.

As mentioned before, the flow regime is another crucial aspect to be considered in the pilot plant design and the scaling process. The recycling pump must be specified in order to ensure the turbulent regime of the flow through the photoreactor [23]. The Reynolds number must be larger than 15,000, and this means that the flow rate must be larger than 24 L/min (for a 32-mm tube diameter). **Table 1** shows the main accessories for hydraulic calculus.

From a simple mechanical energy balance (Bernoulli's equation), the pump theoretical power was estimated (0.241 HP or 179.5 W). The commercially available pump had a nominal power of 0.5 HP with a maximum flow rate of 35 L/min.

4.4.3 Evaluation of real wastewater at pilot solar CPC reactor

A set of pilot plant tests with a simulated mixture of effluent were performed to assess the technical feasibility of heterogeneous photocatalysis for the removal of color from industrial wastewater polluted with a printing dye. The aim was to find suitable conditions for the operation of a larger-scale plan that would allow total discoloration of the industrial effluent. For this purpose, it was considered a robust experimental design. Subsequently, a rate law was obtained, considering the UV accumulated radiation as the independent variable.

The procedure used for the experimental work consisted in treating a constant volume of the diluted mixture with different concentrations of catalyst and fixing the treatment time. The accumulated radiation was measured for sunny and cloudy days in order to observe the solar CPC photoreactor performance under these weather conditions.

The color removal was measured by UV–Vis spectrophotometry, whereby the concentration of the mixture of dyes was indirectly obtained. **Table 2** shows the conditions of the experimental pilot-scale tests.

The experimental results are shown in **Table 3**, and **Figure 16** shows samples collected before and after the photocatalytic treatment. The color was removed entirely, confirming the satisfactory performance of the solar photocatalytic reactor. This evidenced that the chromophore was eliminated. From these results, it was necessary to estimate the size of the full-scale plant for treating 2 m³/d of wastewater. The signal-to-noise ratios for the controllable factors (dilution and catalyst load) are shown in **Table 4**.

	Quantity per meter	K _{eq}
Elbows	15	0.69
Connections	5	0.50
Valve	1	340.00
Tank outlet	1	0.50
Straight pipe	17	—

Table 1.
Fittings and straight pipe of the pilot plant.

Item	Description
Photoreactor	CPC with ten tubes Schott Duran® (32 mm ID)
Area exposed	1.25 m ²
Pump	Centrifugal pump—½ HP of nominal power
Flow rate	32 L/min
Total volume	40 L
Dye composition	Black Flexo: 50% w/w; Basonyl Blue 636®: 50% w/w
Catalyst	Aeroxide® TiO ₂ P-25
Process water	Tap water
Initial pH	7.5
Temperature	25–35°C
Time of tests	10 am to 4 pm

Table 2.
Experimental conditions.

Internal arrangement			External arrangement (Noise)	
Design parameter			UV accumulated radiation (KJ/m ²)	
Exp	[TiO ₂] (g/L)	Dilution	High (>700)	Low (<700)
1	0.4	1:8	89.3%	70.4%
2	0.8	1:8	90.0%	48.4%
3	0.4	1:4	47.4%	29.3%
4	0.8	1:4	91.5%	50.0%

Table 3.
Color removal corresponding to the pilot-scale experiments. © 2009 Walter de Gruyter & Co. Originally published in Colina-Márquez et al. [23] under CC BY-NC-ND 4.0 license.

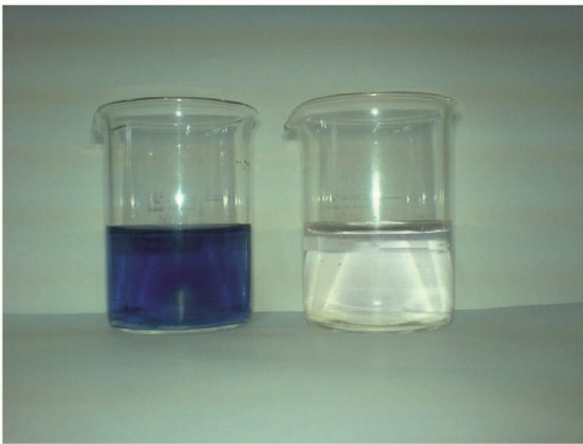


Figure 16.
Samples collected during a typical experiment before (left) and after (right) photocatalytic treatment.

Table 5 showed the experimental data obtained for the color removal respect to the time and the accumulated UV solar radiation. This data was used for fitting parameters of a Langmuir-Hinshelwood modified model, as seen in **Table 6**.

Factor	Level	S/N ratio
Dilution	1:4	32.74
	1:8	36.59
[TiO ₂] g/L	0.4	33.15
	0.8	35.73

© 2009 Walter de Gruyter & Co. Originally published in Colina-Márquez et al. [23] under CC BY-NC-ND 4.0 license.

Table 4.
Signal-to-noise ratio (S/N) for the robust experimental design.

Time (min)	% Discoloration (sunny day)	Q _{uv} , KJ/m ³ (sunny day)	% Discoloration (cloudy day)	Q _{uv} , KJ/m ³ (cloudy day)
−30	0	—	—	—
0	58.1	0	0	0
20	64.5	5493.75	48.3	4481.25
40	71.0	12243.75	51.7	8953.13
60	74.2	18609.38	58.6	13312.50
80	80.7	25734.37	58.6	17690.63
100	83.9	32868.75	62.1	21881.25
120	83.9	40003.12	62.1	25218.75
180	90.4	59765.63	65.5	32681.25
240	90.4	73490.63	65.5	37762.50

Table 5.
Experimental data of the kinetic tests.

Type of day	Apparent rate constant (ppm·KJ/m ³)	Adsorption equilibrium constant (1/ppm)
Sunny	6.506×10^{-2}	3.213×10^{-4}
Cloudy	1.507×10^{-3}	9.419×10^{-3}

Table 6.
Kinetics parameters from Langmuir-Hinshelwood model.

The apparent rate constants seem to be dependent on the accumulated energy and the type of the day. This implies that the color removal will be faster on a sunny day with the same accumulated UV radiation.

Finally, for treating 2 m³/day of contaminated wastewater with a dilution ratio of ratio 1:4, a total of 31 modules of CPC photoreactors were estimated. Nonetheless, during the project development, there were modifications to the design considerations, and 15 modules were implemented at last. An initial isometric drawing is shown in **Figure 17**.

It is important to note that a conical-bottom tank and no secondary storage tank (for clear treated wastewater) were considered at first instance. Nonetheless, the tank was sized to handle 10 m³ per batch, and this was kept until the final design. The conical-bottom tank was selected as the first alternative in order to facilitate the catalyst precipitation and a future removal (when the catalyst was deactivated after several reuses).

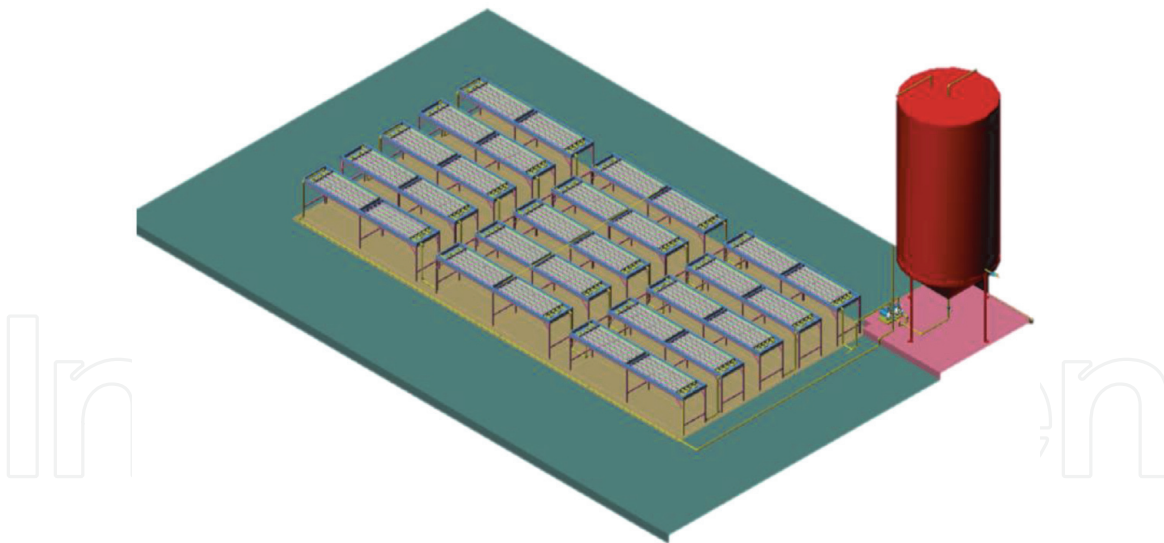


Figure 17.
 Isometric draw of the solar photocatalytic plant with 15 CPC modules.

Two standard plastic tanks were selected for being installed in the solar photocatalytic plant: one of 10 m³, designed for handling the recirculating wastewater, and another one of 4 m³, for storing the treated wastewater. The air-sparging system in the bottom of the recirculation-feed tank was installed in order to maintain the wastewater saturated with oxygen and to avoid limitations in the photocatalytic rate due to the consumption of this chemical species. Moreover, the constant agitation of the water due to the air bubbling helped to maintain the catalyst in suspension and avoid mass transfer limitations because of the solid precipitation during the operation.

The catalyst was settled down after each operation day after turning off the air sparging system. The plant shut down at sunset and the catalyst precipitated overnight. The clear water was transferred to the secondary storage tank and later reused for washing the printing rolls. **Figure 18** shows an overview of the full-scale plant during its first day of steady operation in August 2009.

Currently, this plant is operating at full capacity (4 m³ per day of wastewater). Some other contaminants are being fed to the photocatalytic system; therefore, it was necessary to include a pretreatment consisting of adsorption with activated carbon and a system for adding hydrogen peroxide.

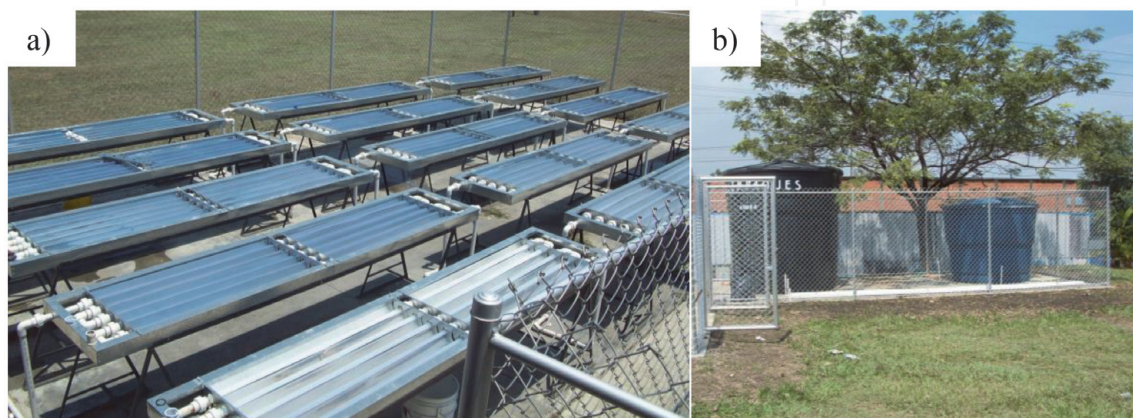


Figure 18.
 Full-scale solar photocatalytic plant for dye-polluted wastewater treatment: (a) CPC photoreactors and (b) recirculation-feed and treated water storage tanks.

IntechOpen

Author details

Gianluca Li Puma¹, Fiderman Machuca-Martínez², Miguel Mueses³,
José Colina-Márquez³ and Ciro Bustillo-Lecompte^{4,5*}

1 Environmental Nanocatalysis and Photoreaction Engineering, Department of
Chemical Engineering, Loughborough University, Loughborough, UK

2 Chemical Engineering School, Universidad del Valle, Ciudadela Universitaria de
Meléndez, Cali, Colombia


3 Chemical Engineering Department, Universidad de Cartagena, Campus de Piedra
de Bolívar, Cartagena de Indias, Colombia

4 Graduate Programs in Environmental Applied Science and Management, Ryerson
University, Toronto, ON, Canada

5 School of Occupational and Public Health, Ryerson University, Toronto, ON,
Canada

*Address all correspondence to: ciro.lecompte@ryerson.ca

IntechOpen

© 2020 The Author(s). Licensee IntechOpen. Distributed under the terms of the Creative Commons Attribution - NonCommercial 4.0 License (<https://creativecommons.org/licenses/by-nc/4.0/>), which permits use, distribution and reproduction for non-commercial purposes, provided the original is properly cited. 

References

- [1] Li Puma G. Dimensionless analysis of photocatalytic reactors using suspended solid photocatalysts. *Chemical Engineering Research and Design*. 2005; **83**(7):820-826. DOI: 10.1205/cherd.04336
- [2] Castilla-Caballero D, Machuca-Martínez F, Bustillo-Lecompte C, Colina-Márquez J. Photocatalytic degradation of commercial acetaminophen: Evaluation, modeling, and scaling-up of photoreactors. *Catalysts*. 2018;**8**(5):179. DOI: 10.3390/catal8050179
- [3] Colina-Márquez J, Machuca-Martínez F, Li Puma G. Photocatalytic mineralization of commercial herbicides in a pilot-scale solar CPC reactor: Photoreactor modeling and reaction kinetics constants independent of radiation field. *Environmental Science & Technology*. 2009;**43**(23):8953-8960. DOI: 10.1021/es902004b
- [4] Braham RJ, Harris AT. Review of major design and scale-up considerations for solar photocatalytic reactors. *Industrial and Engineering Chemistry Research*. 2009;**48**(19): 8890-8905. DOI: 10.1021/ie900859z
- [5] Spasiano D, Marotta R, Malato S, Fernandez-Ibañez P, Di Somma I. Solar photocatalysis: Materials, reactors, some commercial, and pre-industrialized applications. A comprehensive approach. *Applied Catalysis B: Environmental*. 2015;**170-171**:90-123. DOI: 10.1016/j.apcatb.2014.12.050
- [6] Arias F, Ortiz E, López-Vásquez A, Colina-Márquez J, Machuca F. Photocatalytic decolorization of methylene blue with two photoreactors. *Journal of Advanced Oxidation Technologies*. 2008;**11**(1):33-48. DOI: 10.1515/jaots-2008-0104
- [7] Colina-Márquez J, Machuca F, Li Puma G. Radiation absorption and optimization of solar photocatalytic reactors for environmental applications. *Environmental Science & Technology*. 2010;**44**(13):5112-5120. DOI: 10.1021/es100130h
- [8] De Lasa H, Serrano B, Salaices M. Novel photocatalytic reactors for water and air treatment. In: *Photocatalytic Reaction Engineering*. Boston, MA: Springer; 2005. DOI: 10.1007/0-387-27591-6_2
- [9] Ola O, Maroto-Valer MM. Review of material design and reactor engineering on TiO₂ photocatalysis for CO₂ reduction. *Journal of Photochemistry and Photobiology C: Photochemistry Reviews*. 2015;**24**:16-42. DOI: 10.1016/j.jphotochemrev.2015.06.001
- [10] Porta R, Benaglia M, Puglisi A. Flow chemistry: Recent developments in the synthesis of pharmaceutical products. *Organic Process Research and Development*. 2016;**20**(1):12-25. DOI: 10.1021/acs.oprd.5b00325
- [11] Romero RL, Alfano OM, Cassano AE. Cylindrical photocatalytic reactors. Radiation absorption and scattering effects produced by suspended fine particles in an annular space. *Industrial and Engineering Chemistry Research*. 1997;**36**(8): 3094-3109. DOI: 10.1021/ie960664a
- [12] Saravia L. Diseño gráfico de concentradores tipo CPC. *Avances en Energías Renovables y Medio Ambiente*. 2004;**8**(1):25-30. Available from: <https://www.mendoza-conicet.gob.ar/asades/modulos/averma/trabajos/2004/2004-t003-a005.pdf>
- [13] Malato S, Blanco J, Fernández-Alba AR, Agüera A. Solar photocatalytic mineralization of commercial pesticides: Acrinathrin. *Chemosphere*. 2000;**40**(4): 403-409. DOI: 10.1016/S0045-6535(99)00267-2

- [14] Malato S, Blanco J, Vidal A, Richter C. Solar photocatalytic degradation of commercial textile azo dyes: Performance of pilot plant scale thin film fixed-bed reactor. *Applied Catalysis, B: Environmental*. 2002;**37** (1–3):344–352. DOI: 10.1016/j.desal.2008.03.059
- [15] Blanco J, Malato S, Peral J, Sánchez B, Cardona I. Diseño de reactores para fotocátalisis: Evaluación comparativa de las distintas opciones. Chapter 11. In: Blesa M, editor. *Eliminación de Contaminantes por Fotocátalisis Heterogénea*. CYTED: Buenos Aires (Argentina); 2001. pp. 243–266. Available from: <https://www.psa.es/en/projects/solwater/files/CYTED01/17cap11.pdf>
- [16] Dijkstra MFJ, Buwalda H, de Jong AWF, Michorius A, Winkelman JGM, Beenackers AACM. Experimental comparison of three reactor designs for photocatalytic water purification. *Chemical Engineering Science*. 2001;**56**(2):547–555. DOI: 10.1016/S0009-2509(00)00259-1
- [17] Bandala ER, Arancibia-Bulnes CA, Orozco SL, Estrada CA. Solar photoreactors comparison based on oxalic acid photocatalytic degradation. *Solar Energy*. 2004;**77**(5):503–512. DOI: 10.1016/j.solener.2004.03.021
- [18] van Grieken R, Marugán J, Sordo C, Pablos C. Comparison of the photocatalytic disinfection of *E. coli* suspensions in slurry, wall and fixed-bed reactors. *Catalysis Today*. 2009;**144** (1–2):48–54. DOI: 10.1016/j.cattod.2008.11.017
- [19] Romero V, González O, Bayarri B, Marco P, Giménez J, Esplugas S. Degradation of metoprolol by photo-Fenton: Comparison of different photoreactors performance. *Chemical Engineering Journal*. 2016;**283**:639–648. DOI: 10.1016/j.cej.2015.07.091
- [20] Cassano AE, Alfano OM, Brandi RJ, Martín CA. Diseño de reactores para fotocátalisis: conceptos fundamentales. Chapter 10. In: Blesa M, editor. *Eliminación de contaminantes por fotocátalisis heterogénea CYTED*: Madrid; 2001. pp. 201–241. Available from: <https://www.psa.es/en/projects/solwater/files/CYTED01/16cap10.pdf>
- [21] Li Puma G, Yue PL. A laminar falling film slurry photocatalytic reactor. Part II—Experimental validation of the model. *Chemical Engineering Science*. 1998;**53**(16): 3007–3021. DOI: 10.1016/S0009-2509(98)00119-5
- [22] Blanco J, Malato S, Fernández P, Vidal A, Morales A, Trincado P, et al. Compound parabolic concentrator technology development to commercial solar detoxification applications. *Solar Energy*. 1999;**67**(4–6):317–330. DOI: 10.1016/S0038-092X(00)00078-5
- [23] Colina-Márquez J, López-Vásquez A, Díaz D, Rendón A, Machuca-Martínez F. Photocatalytic treatment of a dye polluted industrial effluent with a solar pilot-scale CPC reactor. *Journal of Advanced Oxidation Technologies*. 2009;**12**(1):93–99. DOI: 10.1515/jaots-2009-0111
- [24] Martinez FM, Colina-Márquez JA, Universidad del Valle. Photo-Catalysis Process Applied in Eliminating Recalcitrant Compounds in Industrial Residual Waters. U.S. Patent No. 9,394,186. Washington, DC: U.S. Patent and Trademark Office; 2016. Available from: <https://patents.google.com/patent/US9394186B2/en>